

Near-infrared high refractive-index three-dimensional inverse woodpile photonic crystals generated by a sol-gel process

Baohua Jia,^{a)} Shuhui Wu, Jiafang Li, and Min Gu^{b)}

Centre for Micro-Photonics and CUDOS, Faculty of Engineering and Industrial Sciences, Swinburne University of Technology, Hawthorn, Victoria 3122, Australia

(Received 27 June 2007; accepted 10 September 2007; published online 7 November 2007)

We demonstrate the formation of complete pieces of high refractive-index three-dimensional inverse woodpile photonic crystals by a simple and inexpensive sol-gel process. A mixture of the titanium dioxide precursor and the silica dioxide precursor was infiltrated multiple times into a polymeric template produced by two-photon polymerization to improve the mechanical properties of the inverse structure. After removal of the polymer template, transparent inverse photonic crystals with a refractive index of approximately 2.2 were achieved. The spectroscopic characterization reveals a stop gap in the near-infrared wavelength range, agreeing with the theoretical prediction. © 2007 American Institute of Physics. [DOI: [10.1063/1.2803714](https://doi.org/10.1063/1.2803714)]

The advanced functionalities of three-dimensional (3D) photonic crystal (PC) structures with a complete photonic band gap are vital to the next generation all-optical telecommunications and information systems.^{1,2} Generation of 3D PCs in high refractive-index materials is a necessary condition toward a complete band gap but has remained a challenge with the current fabrication techniques which can be classified as direct and indirect groups. In the case of direct fabrication, electron-beam lithography and etching have been used to produce silicon 3D PCs layer-by-layer.^{3,4} Another layer-by-layer method is based on semiconductor wafer fusion.^{5,6} Although these methods result in precise 3D structures, they are expensive and too complicated for producing arbitrary 3D structures. To address this problem, one has developed a direct laser writing method in high refractive-index materials. It has been shown that 3D PCs can be directly written into chalcogenide glasses⁷ and lithium niobate crystals.⁸ However, direct laser writing in high refractive index material by a high numerical-aperture objective leads to a serious effect of spherical aberration resulting from the refractive index mismatching between the sample and the immersion medium. This effect eventually limits the writing depth to less than 20 μm .⁸

The indirect fabrication of 3D PCs with high refractive index is mainly based on template infiltration. There have been three methods for generating 3D templates. The first type of templates is generated by 3D holography⁹ and the second one by self-assembly.¹⁰ High refractive-index materials such as silicon and titanium dioxide (TiO_2) have been directly infiltrated into these templates,^{9,10} however, lacking of a designing flexibility for arbitrary 3D template structures is the drawback of these methods. Recently the two-photon polymerization (2PP) technique, which enables arbitrary 3D lattice geometries with controllable defects, has been applied in the fabrication of 3D PCs in low refractive-index polymer materials.^{11,12} These 3D polymeric PCs have been used as templates for high refractive-index PCs through a double in-

version approach.¹³ Although high quality PC structures have been achieved, this method involves many complicated chemical steps and expensive instruments. Moreover, double inversion has high requirement of fabrication accuracy thus allows little experimental tolerance. Recently, a single inversion method was introduced to the woodpile template produced by 2PP.¹⁴ Unfortunately, the inverse structure was broken into small pieces during the calcination process due to the poor mechanical strength of the material and the band gap properties were not attainable. In this paper, we demonstrate the generation of complete pieces of high refractive-index inverse woodpile 3D PCs by a simple, inexpensive sol-gel process in which the TiO_2 precursor was mixed with a silica dioxide (SiO_2) precursor to improve the mechanical property of the inverse crystal. The 3D TiO_2 PCs show a refractive index of 2.2 and a stop gap in the near-infrared wavelength region.

3D woodpile templates were fabricated using a photo-sensitive resin SU-8 (MICROCHEM) by the 2PP technique. The fabrication setup was detailed elsewhere.^{14,15} A thin film of SU-8 was illuminated by a tightly focused ultrafast laser beam at a wavelength of 580 nm that was beyond the single-photon absorption band of the resin. A woodpile structure was created by moving the localized focal spot within the film. After fabrication the sample was postbaked and washed out by a SU-8 developer (MICROCHEM) and finally only 3D woodpile structures were left on the cover glass. The structures were designed to be in face-centered-cubic (fcc) geometry. Figure 1 presents scanning electron microscope (SEM) images of a fabricated 3D PC, which has a periodicity of 1 μm and a rod width of approximately 250 nm. A frame (10 μm in width) was fabricated to support the woodpile from collapsing due to the shrinkage occurring during the postprocess.^{16,17} To facilitate the efficient infiltration, a hole 5 μm in width was designed at each wall of the frame [see Fig. 1(a)]. Figure 1(b) shows the magnified structure of Fig. 1(a).

To form the inverse structures, a solution of precursor titanium propoxide $\text{Ti}(\text{OR})_4$ (Aldrich) was used as a main infiltration liquid, which can be transferred into TiO_2 through

^{a)} Author to whom correspondence should be addressed. Electronic mail: bjia@swin.edu.au

^{b)} Electronic mail: mgu@swin.edu.au

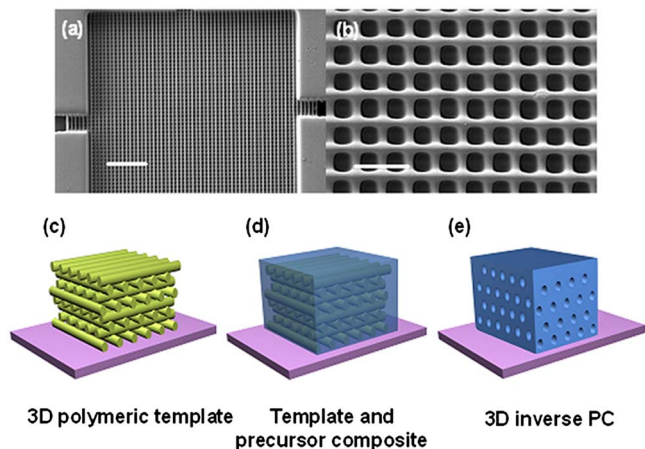


FIG. 1. (Color online) (a) SEM image of a SU-8 template (lattice constant $a=1.0 \mu\text{m}$) fabricated by 2PP. A hole was formed at each frame to facilitate the efficient infiltration. Scale bar: $10 \mu\text{m}$. (b) A magnified image of (a) showing the detailed structure of the PC. Scale bar: $2 \mu\text{m}$. (c)–(e) Schematic diagrams illustrating the steps of the infiltration process to get an inverse 3D PC.

a sol-gel process. One major hurdle previously had in this approach was the poor mechanical property of the nanoporous TiO_2 preventing one to obtain even a complete piece of inverse PC.¹⁴ To overcome this problem and improve the strength and transparency of the ultimate replica, SiO_2 , a material with good mechanical property, is incorporated into TiO_2 by mixing a small amount of precursor silica propoxide $\text{Si}(\text{OR})_4$ (Aldrich) into the titanium propoxide with a mole ratio of 10:1 between $\text{Ti}(\text{OR})_4$ and $\text{Si}(\text{OR})_4$. The two precursors mixed in molecular level. Both of them undergo a sol-gel process and cocondense into one homogeneous network instead of forming interpenetrated two networks. The resultant SiO_2 has a similar structure as TiO_2 . After mixing with SiO_2 a refractive index of approximately 2.2 can be expected for the final replica. Another important factor contributing to the previous broken piece was the strong tension occurs during a fast sol-gel process. To avoid this, another solvent toluene instead of ethanol¹⁴ was selected because the former has lower templating hydrophilicity and a higher boiling point, which can reduce the reaction speed of the sol-gel process, thus leading to a uniform shrinkage when the precursor condenses to TiO_2 , though the volume of the composite reduces dramatically by a factor of 4 owing to an increase in the density of the material. As a result, crack-free inverse structures can be generated.

Figures 1(c)–1(e) illustrate the procedure to achieve the inverse structure. A concentrated (80 vol %) solution of the precursors was injected onto the surface of the template (degassed) and then infiltrated into the space of the woodpile structures. To facilitate the sol-gel process the composites were exposed in air for at least 24 h. To remove the polymeric templates and minimize the induced tension, the composites were heated to $270 \text{ }^\circ\text{C}$ by increasing the temperature with a step of $50 \text{ }^\circ\text{C}$ and each step lasted for 30 min. During this process the sol-gel process can be completed while the polymeric template still remains stable as the cross-linked SU-8 template decomposes at $380 \text{ }^\circ\text{C}$. The sample was then cooled down to the room temperature allowing for multiple infiltrations to completely fill the space of the woodpile tem-

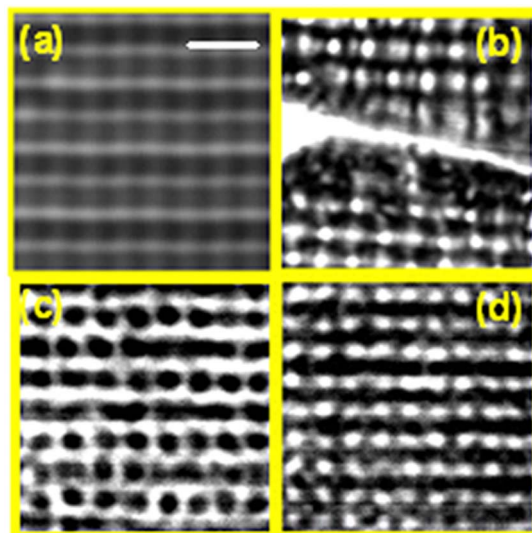


FIG. 2. (Color online) Confocal microscopic images of (a) a SU-8 template ($a=1.0 \mu\text{m}$); (b) a broken piece of the inverse PC due to the absence of SiO_2 in the final replica; (c) and (d) complete pieces of the inverse woodpile PCs [(c) $a' \approx 0.95 \mu\text{m}$ and (d) $a' \approx 0.84 \mu\text{m}$]. Scale bar: $2 \mu\text{m}$.

plate thus minimizing the shrinkage caused by the dramatic mass loss during the heating process. Finally, the infiltrated sample was heated up quickly to $250 \text{ }^\circ\text{C}$ for 10 min and then to $490 \text{ }^\circ\text{C}$ for 2.5 h to completely remove the polymeric template.

To observe the inner structure of the resultant 3D inverse woodpile PCs, we adopted a confocal reflection microscope (IX70, Olympus) with an objective of numerical aperture 1.4 rather than the SEM because the former is noninvasive.¹⁸ Figures 2(a)–2(d) present the confocal optical sections of the template and the inverse 3D PCs along the vertical direction. As expected, the image contrast of the inverse structures [Figs. 2(b)–2(d)] is higher than that of the template [Fig. 2(a)]. It can be seen in Fig. 2(b) that without adding SiO_2 the inverse PC broke into pieces. After the SiO_2 precursor was used, complete pieces of inverse PCs were achieved [Figs. 2(c) and 2(d)]. Although the lattices are slightly distorted due to the calcination process, the periodic arrangements of the lattices are clearly evident. A lattice constant (a' for inverse structures) of approximately $0.95 \mu\text{m}$ was found in the inverse structure in Fig. 2(c), which agrees well with the lattice spacing of the template [Fig. 2(a), $a=1.0 \mu\text{m}$] providing that a slight shrinkage caused by the calcinations is considered. The experimental result was almost completely reproducible provided that each step of the temperature control is accurately followed. This is confirmed in Fig. 2(d) in which another complete piece of the inverse structure with a lattice constant $a'=0.84$ is presented.

To investigate the photonic band gap properties of the inverse 3D PCs, a Fourier-transform infrared (FTIR) spectrometer (Thermo Nicolet) in conjunction with an infrared microscope (Continuum) was employed.¹⁶ The reflective objective of the microscope (Relechromat) provides a hollow light cone varying from 18° to 41° with respect to the surface normal (ΓX) of the PC resulting in an averaged measurement of the transmission. The transmission spectra of the inverse PCs and a polymer template with a lattice constant of

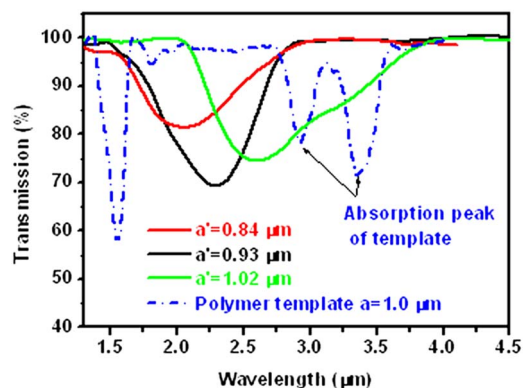


FIG. 3. (Color online) FTIR measurement of the transmission spectra of a SU-8 template (dotted curve) and inverse woodpile structures with different lattice constants in the stacking direction (ΓX).

1.0 μm , measured in the ΓX direction, are shown in Fig. 3. As expected, a partial band gap at a wavelength of 1.6 μm is observed in the polymer template, which agrees well with the theoretical predication ($n_{\text{SU-8}}=1.56$). The replica of this structure possesses a broad stop gap with more than 30% suppression in transmission at a longer wavelength (2.28 μm) because of the increase of the refractive-index contrast. Two polymer absorption at the wavelengths of 2.8 and 3.3 μm in the transmission spectrum of the polymer template do not occur to the spectra of the inverse 3D PCs, indicating that the template was completely removed by the calcination. The three inverse woodpile PCs with lattice constants of 0.84, 0.93, and 1.02 μm (a 7% decrease in the lattice constant caused by shrinkage was considered here) show partial band gaps at wavelengths 2.04, 2.28, and 2.58 μm , respectively (Fig. 3). A linear dependence of the midgap wavelength of the stop gap on lattice constant was found, as predicted, which demonstrates a good reproducibility of the fabrication method.

To estimate the refractive index of the replica obtained in the experiment, we calculate the band gap position as a function of the lattice constant for different refractive indices using the MPB software package.¹⁹ An inverse woodpile with a fcc geometry was considered. As shown in Fig. 4, the experimental dependence of the midgap wavelength as a function of the lattice constant fits well the theoretical prediction

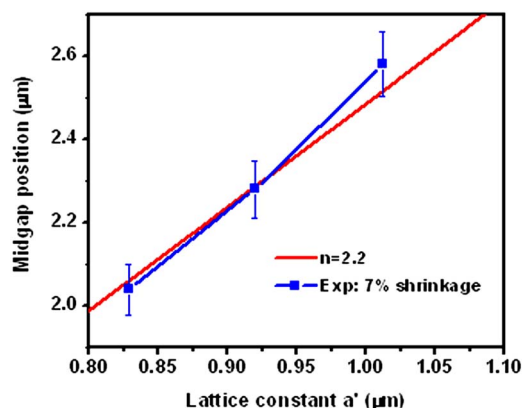


FIG. 4. (Color online) Experimental (Exp) and theoretical midgap positions as a function of the lattice constant a' for inverse PCs with a refractive index of 2.2.

for refractive index 2.2, agreeing well with the expected refractive index of the mixture of TiO_2 and SiO_2 . Such a refractive index may facilitate a complete band gap feature.²⁰ However, due to the slight imperfection (disorder) of the periodic structures induced by the calcination and the broad detection angle of FTIR which averages the transmission in different directions and leads to the less suppression within the stop gap, no complete band gap has been observed from the inverse woodpile structures. The distortion could be improved by a finer control of the temperature which was limited by our instrument. The fulfillment of a complete piece of the TiO_2 inverse 3D woodpile PC is a critical step toward a large complete band gap, when a higher temperature (>700 $^\circ\text{C}$) annealing process is applied to the inverse structure to facilitate the change of the TiO_2 from the anatase phase to the high refractive-index rutile phase ($n=2.7$).²¹

In conclusion, using a sol-gel process, complete pieces of high refractive-index 3D inverse woodpile PCs with stop gaps at the near-infrared wavelength range were achieved. By introducing SiO_2 precursors into the system the mechanical property of the resultant PCs were improved. The use of multiple infiltrations has led to minimum shrinkage of the inverse structures. A high refractive index of 2.2 was obtained in the final replica. The demonstrated method is simple and inexpensive to generate arbitrary 3D high refractive-index PCs with functional defects.

This work was produced with the assistance of the Australian Research Council under the ARC Centres of Excellence program. The Centre for Ultrahigh-bandwidth Devices for Optical Systems (CUDOS) is an ARC Centre of Excellence.

- ¹E. Yablonovitch, Phys. Rev. Lett. **58**, 2059 (1987).
- ²S. John, Phys. Rev. Lett. **58**, 2486 (1987).
- ³S. Y. Lin, J. G. Fleming, D. L. Hetherington, B. K. Smith, R. Biswas, K. M. Ho, M. M. Sigalas, W. Zubrzycki, S. R. Kurtz, and J. Bur, Nature (London) **394**, 251 (1998).
- ⁴M. Qi, E. Lidorikis, P. Rakich, S. G. Johnson, J. D. Joannopoulos, E. P. Ippen, and H. I. Smith, Nature (London) **429**, 538 (2004).
- ⁵S. Noda, K. Tomoda, N. Yamamoto, and A. Chutinan, Science **289**, 604 (2000).
- ⁶S. Ogawa, M. Imada, S. Yoshimoto, M. Okano, and S. Noda, Science **305**, 227 (2004).
- ⁷S. Wong, M. Deubel, F. Perez-Willard, S. John, G. A. Ozin, M. Wegener, and G. V. Freymann, Adv. Mater. (Weinheim, Ger.) **18**, 265 (2006).
- ⁸G. Zhou and M. Gu, Opt. Lett. **31**, 2783 (2006).
- ⁹M. Campbell, D. N. Sharp, M. T. Harrison, R. G. Denning, and A. J. Turberfield, Nature (London) **404**, 53 (2000).
- ¹⁰A. Blanco, E. Chomski, S. Grabchak, M. Ibisate, S. John, S. Leonard, C. Lopez, F. Mesguer, H. Miguez, J. Mondia, G. A. Ozin, O. Toader, and H. V. Driel, Nature (London) **405**, 437 (2000).
- ¹¹H.-B. Sun, S. Matsuo, and H. Misawa, Appl. Phys. Lett. **74**, 786 (1999).
- ¹²M. Deubel, G. Von Freymann, M. Wegener, S. Pereira, K. Busch, and C. M. Soukoulis, Nat. Mater. **3**, 444 (2004).
- ¹³N. Tetreault, G. V. Freymann, M. Deubel, M. Hermatschweiler, F. Perez-Willard, S. John, M. Wegener, and G. A. Ozin, Adv. Mater. (Weinheim, Ger.) **18**, 457 (2006).
- ¹⁴J. Serbin, A. Ovsianikov, and B. Chichkov, Opt. Express **12**, 5221 (2004).
- ¹⁵B. Jia, X. Gan, and M. Gu, Optik (Stuttgart) **115**, 358 (2004).
- ¹⁶M. Straub and M. Gu, Opt. Lett. **27**, 1824 (2002).
- ¹⁷B. Jia, J. Li, and M. Gu, Aust. J. Chem. **60**, 484 (2007).
- ¹⁸M. J. Ventura, M. Straub, and M. Gu, Appl. Phys. Lett. **82**, 1649 (2003).
- ¹⁹S. Johnson and J. Joannopoulos, Opt. Express **8**, 173 (2001).
- ²⁰K. M. Ho, C. T. Chan, C. M. Soukoulis, R. Biswas, and M. Sigalas, Solid State Commun. **89**, 413 (1994).
- ²¹J. E. G. J. Wijnhoven and W. L. Vos, Science **281**, 802 (1998).